Vibrio parahaemolyticus orchestrates a multifaceted host cell infection by induction of autophagy, cell rounding, and then cell lysis

Dara L. Burdette*†, Melanie L. Yarbrough*†, Anthony Orvedahl‡, Christopher J. Gilpin§ and Kim Orth*¶

Departments of *Molecular Biology, ‡Internal Medicine and Microbiology, and §Cell Biology, University of Texas Southwestern Medical Center, Dallas, TX 75390

Edited by Eric N. Olson, University of Texas Southwestern Medical Center, Dallas, TX, and approved June 19, 2008 (received for review March 21, 2008)

The bacterial pathogen *Vibrio parahaemolyticus* utilizes a type III secretion system to cause death of host cells within hours of infection. We report that cell death is completely independent of apoptosis and occurs by a mechanism in which injection of multiple type III effectors causes induction of autophagy, cell rounding, and the subsequent release of cellular contents. Autophagy is detected by the appearance of lipidated light chain 3 (LC3) and by increases in punctae and vacuole formation. Electron microscopy reveals the production of early autophagic vesicles during infection. Consistent with phosphoinositide 3 (PI3) kinase playing a role in autophagy, treatment of infected cells with a PI3 kinase inhibitor attenuates autophagy in infected cells. Because many effectors are injected during a *V. parahaemolyticus* infection, it is not surprising that the presence of a sole PI3 kinase inhibitor does not prevent inevitable host-cell death. Our studies reveal an infection paradigm whereby an extracellular pathogen uses its type III secretion system to cause at least three parallel events that eventually result in the proinflammatory death of an infected host cell.

host-pathogen | type III secretion | apoptosis | effector | inflammatory

Vibrio parahaemolyticus is a Gram-negative bacterium commonly found in marine and estuarine environments (1). Infection leads to acute gastroenteritis and typically results from consumption of contaminated shellfish. Individuals who are immune-compromised or burdened with preexisting health conditions are at high risk for severe complications that can result in death (2). This bacterium has become increasingly important because pandemic strains are emerging throughout the world (1, 2). *V. parahaemolyticus* also has been found along coastal waters and within fish farms in the United States (1, 2). *V. parahaemolyticus* infection is a major health and economic issue in Southeast Asia. Problems associated with *V. parahaemolyticus* infections in the United States are believed to be largely underdiagnosed and may represent a major health risk. Therefore, a better understanding of the virulence mechanisms of *V. parahaemolyticus* is essential for better diagnosis, treatment, and prevention of infections.

The thermostable direct hemolysin (TDH) and the thermostable-related hemolysin (TRH) are the best-characterized virulence factors from this bacterium. TDH and TRH are reversible amyloid toxins that cause β-hemolysis on Wagatsuma agar, known as the "Kanagawa phenomenon." However, infection with Δ*tdh* and Δ*trh* strains of *V. parahaemolyticus* results in rapid and acute cell death in a tissue culture model (3). This cell death is associated with the presence of a type III secretion system (T3SS) (3). Bacterial T3SSs deliver proteins, called "effectors," into the cytosol of host cells during infection (4). Although the T3S machinery often is conserved among gram-negative pathogens, the effectors from each system differ widely in their mechanism of action. These effectors, like viral oncoproteins, are potent molecules that mimic or capture an endogenous eukaryotic activity to disrupt the cellular response to infection (5, 6).

Sequencing of the genome of the RIMD2210633 strain of *V. parahaemolyticus* revealed the presence of two T3SSs, 1 encoded on chromosome I (T3SS1) and the other on chromosome 2 (T3SS2). T3SS2 is found only in clinical isolates of *V. parahaemolyticus* and is associated with enterotoxicity in a rabbit ileal loop model (7). We have shown that the effectors VopA and VopL from T3SS2 disrupt innate immunity and the actin cytoskeleton, respectively (8, 9). However, mutant strains unable to secrete proteins from T3SS2 are cytotoxic to cells, suggesting a role for T3SS1 in virulence (3, 8). Genotyping has shown that all isolates of *V. parahaemolyticus* harbor T3SS1, which resembles the T3SS of *Yersinia spp.* in structure and organization, although there is no similarity between their predicted effectors (7, 10). Although the cytotoxic effects caused by T3SS1 during infection are thought to occur by apoptosis, the mechanism of cell death is not well established (11, 12).

In this article, we describe a mechanism used by *V. parahaemolyticus* to cause cell death. We demonstrate that the T3SS-mediated infection initiates with the activation of acute autophagy, followed by cell rounding, and concludes with the lethal release of cellular contents. We hypothesize that this proinflammatory, multifaceted infection benefits the invading bacteria, allowing *V. parahaemolyticus* to capitalize on the release of cellular nutrients.

Results

Infection with *Vibrio* Strain POR3 Induces Rapid Cytotoxicity in Multiple Cell Types. To develop a better understanding of the mechanism of cell death induced by *V. parahaemolyticus*, we infected HeLa cells and RAW 264.7 macrophages with several different *Vibrio* strains designated POR1, POR2, and POR3. The parental POR1 strain possesses both T3SSs but lacks genes for TDH and TRH. Two isogenic strains derived from the POR1 strain were used to dissect the phenotype caused by each T3SS. These strains are incapable of secreting effectors from either T3SS1 (POR2) or T3SS2 (POR3) (3). POR1 induces cytotoxicity in both the HeLa cells and RAW 264.7 macrophages [supporting information (SI) Fig. S1 *C* and *D*]. The strain lacking T3SS1 (POR2) is unable to induce a lethal phenotype, but obvious changes in the actin cytoskeleton are observed (Fig. S1 *E* and *F*) (8). Infection with a strain lacking T3SS2 (POR3) causes a cytotoxic pheno-

Author contributions: D.L.B., M.L.Y., and K.O. designed research; D.L.B., M.L.Y., and C.J.G. performed research; A.O. and C.J.G. contributed new reagents/analytic tools; D.L.B., M.L.Y., A.O., C.J.G., and K.O. analyzed data; and D.L.B., M.L.Y., A.O., and K.O. wrote the paper.

The authors declare no conflict of interest.

This article is a PNAS Direct Submission.

†D.L.B. and M.L.Y. contributed equally to this work.

¶To whom correspondence should be addressed. E-mail: kim.orth@utsouthwestern.edu.

This article contains supporting information online at www.pnas.org/cgi/content/full/0802773105/DCSupplemental.

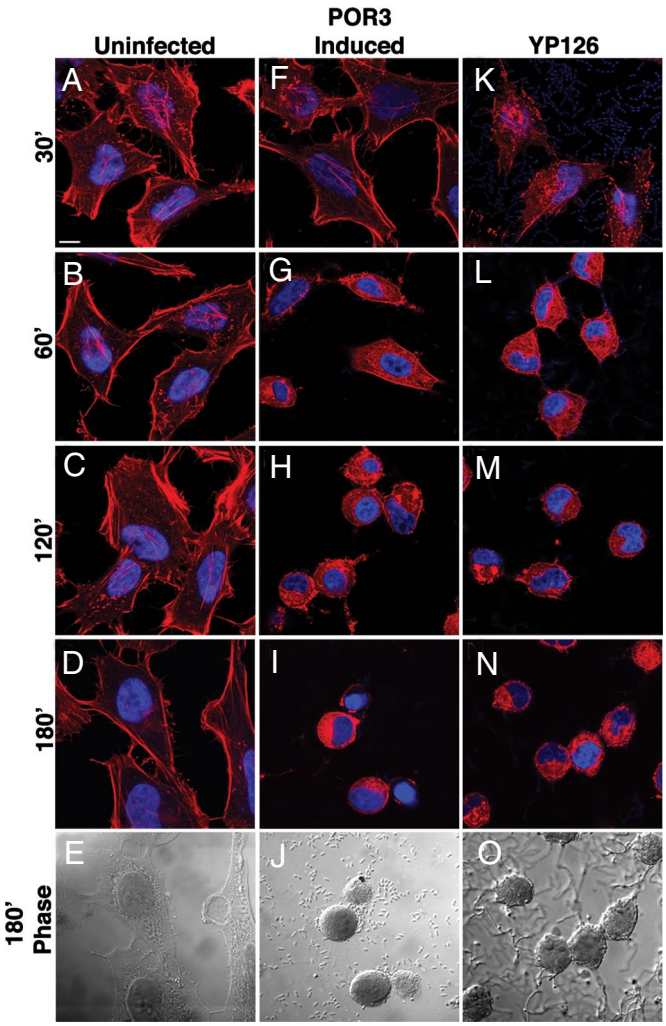

Fig. 1. POR3 infection induces rapid cytotoxicity in HeLa cells. POR3 and YP126 grown in T3S-inducing conditions were used to infect HeLa cells as described. Cells were uninfected (*A–E*) or were infected with induced POR3 (*F–J*) or with YP126 (*K–O*). Cells were visualized using confocal microscopy using rhodamine phalloidin to stain actin (red) and Hoechst to stain nuclei (blue). (Scale bar represents 10 μm.)

type similar to that seen in POR1-infected cells (Fig. S1 *G* and *H* and *C* and *D*, respectively). Some of the T3SSs can be induced before infection by growing the bacteria at a higher temperature and with decreased calcium, resulting in an acceleration of the T3SS1-dependent cytotoxic phenotype (Fig. S2). These conditions are similar to those used for inducing the T3SS of *Yersinia spp.* (13). Cells infected with the induced POR3 strain exhibit cytotoxicity as early as 60 min after infection, with only cell fragments observed at 3 h after infection (Fig. S2 *B–E* and *K–N*). Infection with the uninduced POR3 strain slows the death process, allowing observation of the T3SS1-induced cell death over an extended interval (Fig. S2 *F–I* and *O–R*). These data support the hypothesis that cytotoxicity is a result of infection with T3SS1, and the remaining experiments described in this study use the POR3 strain to decipher the mechanism used by T3SS1 to induce rapid cytotoxicity.

T3SS1-Induced Cytotoxicity Does Not Depend on Caspase Activation. Cells infected with POR3 exhibit morphology consistent with apoptotic death, including cell rounding and nuclear shrinkage (Fig. 1 *F–J*) (14). This phenotype resembles that seen for cells infected with *Yersinia pseudotuberculosis* (YP126), an extracellular bacterium that induces apoptosis in infected cells (Fig. 1 *K–P*) (15). To test whether *V. parahaemolyticus* induces cell death by apoptosis, we assayed infected RAW 264.7 macrophages for the activation of caspases. Although caspase activity is elevated in YP126-infected or staurosporine-treated cells, POR3-infected macrophages do not show any evidence of caspase 3/7 activation (Fig. 2*A*). In addition, polyADP ribose polymerase (PARP), a downstream target of caspase 3, is cleaved in both staurosporine-treated cells and *Yersinia*-infected cells (Fig. 2*B*, lanes 7–9 and 10–12, respectively) but not in POR3-infected cells (Fig. 2*B*, lanes 4–6). Based on these observations, we conclude that POR3-induced cytotoxicity is independent of apoptotic machinery.

POR3-Induced Cytotoxicity Leads to Release of Cellular Contents. Apoptosis is a noninflammatory type of cell death, whereas other forms of death such as necrosis are proinflammatory (16). To investigate the type of cell death that POR3 causes, we analyzed whether cellular contents are released during infection by measuring the release of lactate dehydrogenase (LDH). We observed elevated levels of cytoplasmic LDH released into the media during infection of macrophages with the POR3 strain, indicating that the integrity of the host-cell membrane is compromised (Fig. 2*C*). As expected, cells in which apoptotic death was induced by *Yersinia* infection or staurosporine treatment exhibited no increase in LDH release (Fig. 2*C*). Furthermore, analysis of LDH release in the presence of 5 mM glycine did not affect the levels of LDH released from POR3-infected HeLa cells, thereby eliminating pyroptosis as a possible mechanism for cell death (data not shown) (16–20). Consistent with our previous findings on cytotoxicity, the induced POR3 strain caused LDH release faster than the uninduced POR3 strain (2 and 3 h, respectively, Fig. 2*C*). In total, these results support the hypothesis that *V. parahaemolyticus* T3SS1-mediated cytotoxicity is not caused by apoptosis and that the infection is proinflammatory because of the release of cellular contents.

***V. parahaemolyticus* Infection Rapidly Induces T3SS1-Dependent Autophagy.** Autophagy is a cellular pathway that has been linked to cell fate and involves the sequestration of cytoplasmic contents in double-membraned autophagosomes that are delivered to lysosomes for degradation (14, 21). To examine the potential role of autophagy in T3SS1-dependent cytotoxicity, we monitored a marker of autophagic vesicle formation, LC3, using microscopic and biochemical indicators (22). Induction of autophagy results in incorporation of LC3 into autophagic vesicles (22). We generated a HeLa cell line that stably expresses GFP-LC3 to assess the formation of autophagic vesicles by fluorescent microscopy (22). As a positive control, cells were starved in the presence of protease inhibitors to activate autophagy. Over the course of 3 h, GFP-LC3 punctae accumulated slowly in starved cells to levels above those in untreated cells (Fig. 3 *G–I* and *A–C*, respectively). By contrast, the formation of autophagic vesicles in POR3-infected cells was rapid, occurring within 1 h after infection and increasing dramatically over the next 2 h (Fig. 3 *D–F*). To confirm that cells infected with the POR3 strain were inducing autophagy, the infected cells were analyzed by electron microscopy. The POR3-infected cells contained multiple autophagic vesicles that had engulfed cytoplasm, organelles, membranes, and smaller vesicles (Fig. 3 *J–M*).

To test T3SS1-dependent activation of autophagy further, we used a biochemical indicator for autophagy that monitors a posttranslational modification of LC3. Cytosolic LC3 (LC3-I) is targeted to newly forming autophagosomes by lipidation with phosphatidylethanolamine via an ubiquitin-like conjugation system, resulting in the formation of membrane-associated LC3-II (23, 24). In a cell line stably expressing a GFP-tagged LC3,

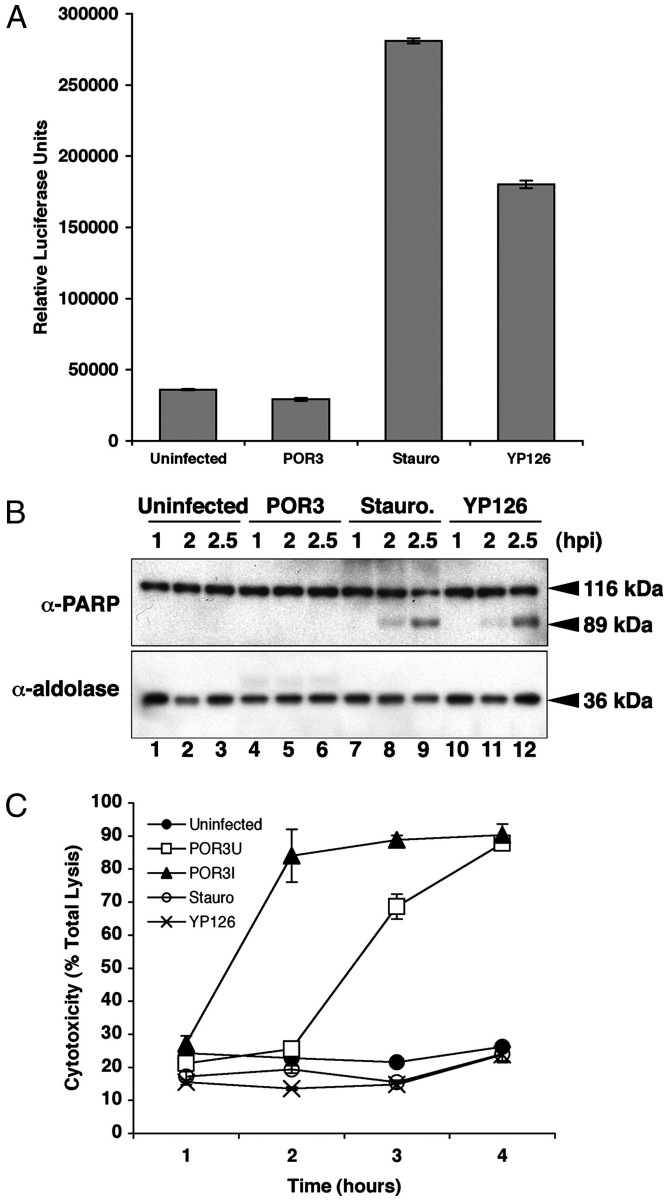

Fig. 2. T3SS1-dependent cytotoxicity is not caused by apoptosis. (*A*) RAW 264.7 macrophages were infected with POR3 for 2.5 h. Cells were treated with 1 μM staurosporine (Stauro) or infected with YP126 as positive controls. After infection, cells were lysed and normalized for protein content. Caspase 3/7 activation was measured by luminescence with the Caspase-Glo assay. (*B*) RAW 264.7 macrophages were treated identically as described in *A* (uninfected, lanes 1–3; POR3, lanes 4–6; Stauro, lanes 7–9; or YP126, lanes 10–12). Cells were lysed at the indicated time points as described and immunoblotted with anti-PARP antibody or anti-aldolase antibody to confirm equal loading. (*C*) Cytotoxicity of RAW 264.7 macrophages was measured by LDH release. Cells were infected as described over a time course with POR3 grown in T3S-inducing conditions (POR3I, closed triangle) or in noninducing conditions (POR3U, open square). Cells were left uninfected (closed circle), infected with YP126 (×) or treated with 1 μM staurosporine (open circle) as controls. Cytotoxicity was calculated as a percent of total lysis of cells that were lysed in Triton X-100.

LC3-II accumulates slowly during amino acid starvation in the presence of lysosomal protease inhibitors, as evidenced by the production of the more rapidly migrating LC3-II in SDS/PAGE (Fig. 3*N*, lanes 7–9, and *P*). In cells infected with uninduced POR3 strain, GFP-LC3-II accumulates rapidly within 1 h and continues to be the dominant form throughout infection

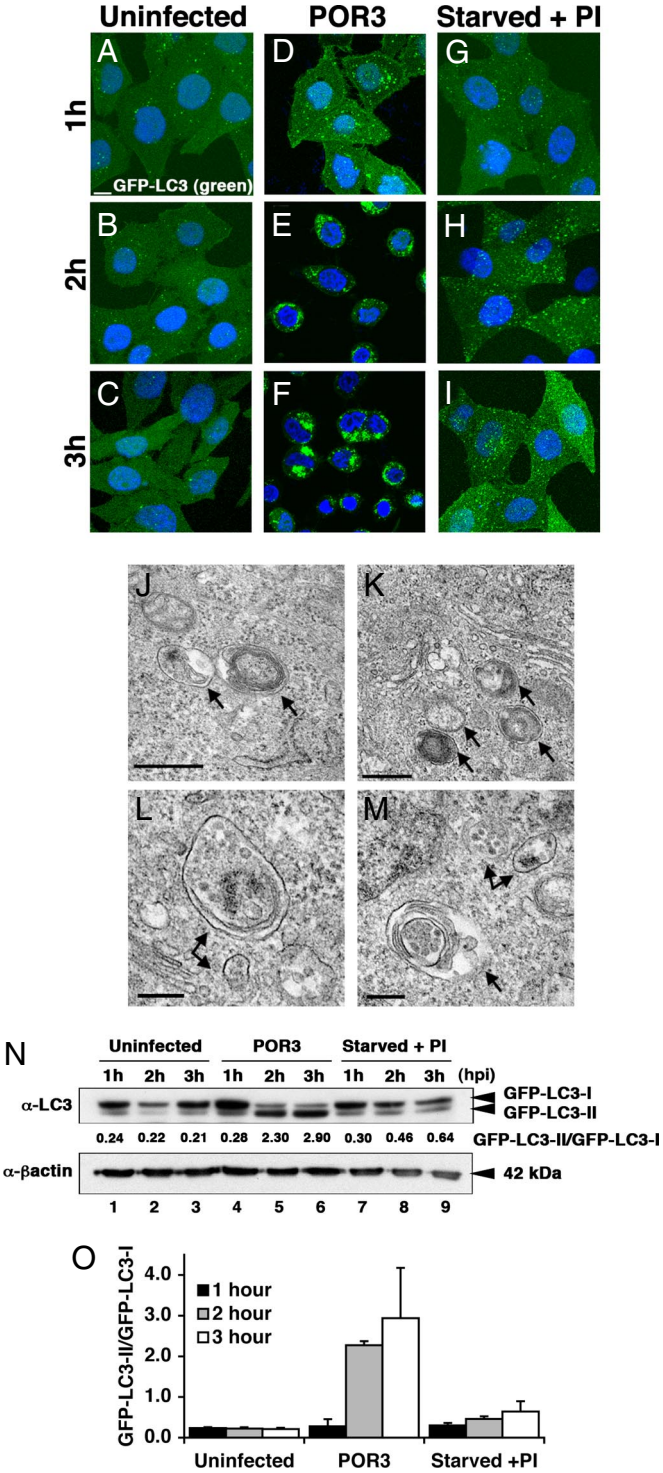

Fig. 3. *V. parahaemolyticus* induces autophagy. (*A–I*) GFP-LC3 HeLa cells were plated on coverslips and left uninfected (*A–C*), infected with POR3 (*D–F*), or starved with protease inhibitors (PI) (*G–I*) for 1, 2, and 3 h. Samples were prepared for microscopy at 1-h time points as described. (Scale bar = 10 μm.) (*J–M*) HeLa cells were infected with POR3 as described, harvested 2 h after infection, and processed for electron microscopy as described in *Materials and Methods*. Arrows designate early autophagosomes. (Scale bars = 0.5 μm in *J* and *K* and 0.2 μm in *L* and *M*.) (*N*) GFP-LC3 HeLa cells were left uninfected (lanes 1–3), infected with *V. parahaemolyticus* POR3 (lanes 4–6), or starved with protease inhibitors (PI) (lanes 7–9) for 1, 2, and 3 h. Samples were immunoblotted using anti-LC3 and anti-β-actin antibodies. (*O*) Relative LC3-II accumulation was determined as described. The data are the means ± SD from three independent experiments.

MICROBIOLOGY

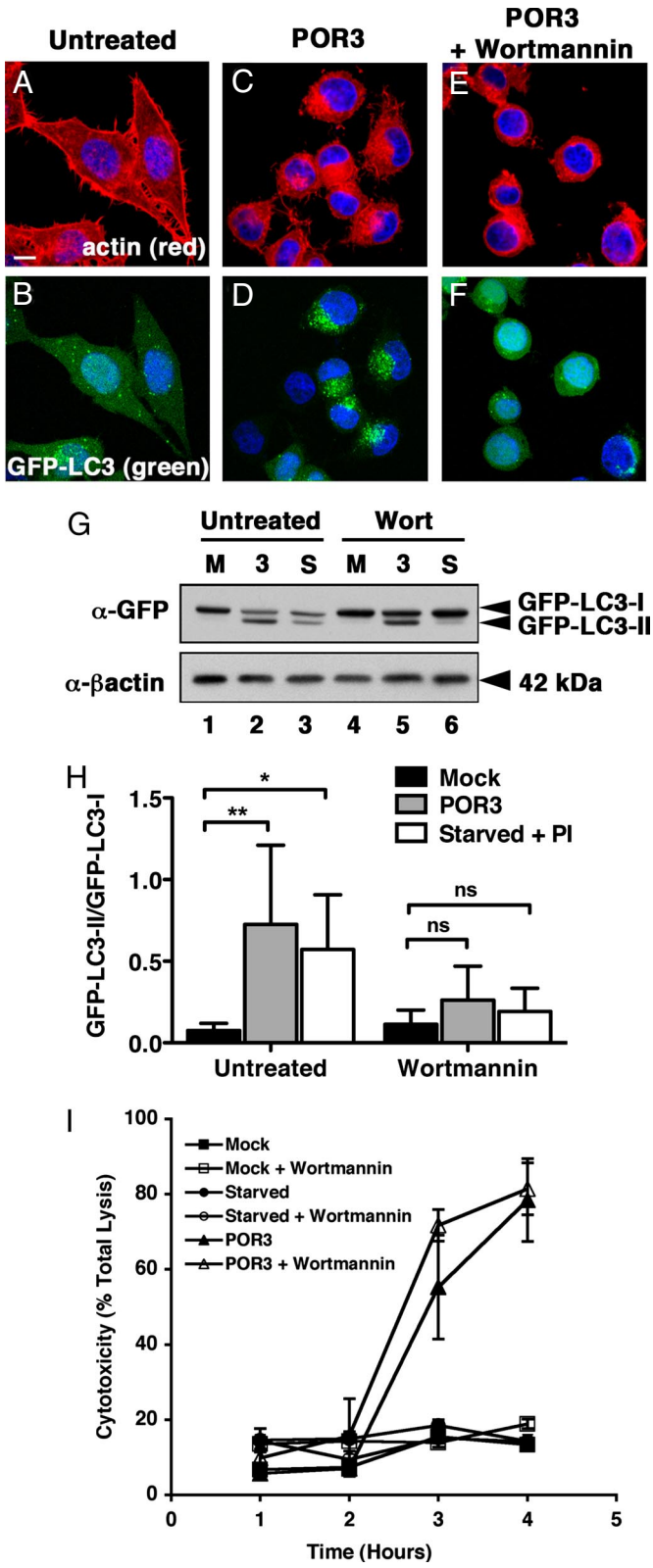

Fig. 4. Inhibitors of PI3 kinase prevent *V. parahaemolyticus*–induced autophagy. (*A–F*) GFP-LC3 HeLa cells were untreated (*A* and *B*) or infected with POR3 in the absence (*C* and *D*) or presence (*E* and *F*) of 10 μM wortmannin for 2 h. Cells were visualized using confocal microscopy as described. (Scale bar = 10 μm.) (*G*) GFP-LC3 HeLa cells were uninfected (M, lanes 1 and 4), infected with *V. parahaemolyticus* POR3 (3, lanes 2 and 5), or starved with protease inhibitors (PI) (S, lanes 3 and 6) in the absence (lanes 1–3) or presence (lanes 4–6) of 10 μM wortmannin for 2 h. Samples were immunoblotted with anti-GFP and anti-β-actin antibodies. (*H*) Relative LC3-II accumulation was determined as described. The data are the means ± SD from five independent experiments. *, $P < 0.05$; **, $P < 0.01$; ns, not significant by two-way ANOVA, Bonferroni posttest. (*I*) Cytotoxicity over time of uninfected (squares), starved (circles), or POR3-infected (triangles) HeLa cells in the absence (closed symbols) or presence of 10 μM wortmannin (open symbols).

(Fig. 3*N*, lanes 4–6, and *P*). These studies parallel the timing of our microscopic observations of punctae formation (Fig. 3 *A–I*) and autophagic vesicle accumulation (Fig. 3 *J–M*). Consistent with our hypothesis that autophagy depends on T3SS1, only the POR1 and POR3 strains induce conversion of LC3, whereas a T3SS1-negative strain (POR2) does not (Fig. S3). Our microscopic and biochemical studies support the hypothesis that infection with *V. parahaemolyticus* induces acute and rapid autophagy before the release of cellular contents, because the accumulation of GFP-LC3 punctae and the conversion of LC3-I to LC3-II (Fig. 3) precede the release of LDH (Fig. 2*C*) during infection with the uninduced POR3 strain.

Inhibitors of PI3 Kinase Prevent T3SS1-Induced Autophagy but Not Cell Death. An early step in the autophagy pathway involves the activation of PI3 kinases, and treatment of starved cells with PI3 kinase inhibitors prevents autophagy (25). We used the PI3 kinase inhibitor wortmannin to test whether *V. parahaemolyticus* induces autophagy using known cellular mechanisms (26). Treatment of infected cells with wortmannin inhibits autophagy in *V. parahaemolyticus*–infected cells, as indicated by a dramatic reduction of GFP-LC3 punctae (Fig. 4*F*). Coincident with the decrease in punctae, we observe a decrease in LC3-II accumulation [Fig. 4*G* (compare lanes 2 and 5) and *H*]. Based on these studies, we predict that acute T3SS1-induced activation of autophagy occurs proximal to, or at the point of, the activation of PI3 kinases. The treatment with this PI3 kinase inhibitor did not rescue the infected cells from death, probably because of the activation of signaling pathways by other T3SS effectors that cause cell rounding and lysis and are not susceptible to this chemical inhibitor (Fig. 4 *E* and *I*).

Discussion

Herein, we present a paradigm used by an extracellular pathogen, *V. parahaemolyticus*, to induce cell death methodically and efficiently. This process is independent of classical apoptotic machinery. We observe a multifaceted phenotype in infected cells by which multiple, albeit temporally orchestrated, mechanisms eventually culminate in the efficient death of host cells within hours of infection (Fig. 5). Upon infection, we observe the T3SS1-mediated activation of autophagy, both microscopically and biochemically. We then observe a dramatic rounding of the host cell, undoubtedly caused by changes in the cytoskeleton of the infected cell. After both of these steps, we observe the release of cellular contents. We propose that *V. parahaemolyticus* could use T3SS1 to mediate this multifaceted mechanism both to capitalize on the release of these nutrients and to defend itself against phagocytosis by immune cells responding to proinflammatory signals at the site of infection (Fig. 5).

The T3SS1 is found in both environmental and pathogenic strains of *V. parahaemolyticus* (10). During infection of an incidental host, such as humans, this type of acute death induced by T3SS1 could work in favor of the pathogen. Similarly, *V. parahaemolyticus*'s survival in the environment might be secured by its ability to hijack nutrients from other living cells or, possibly, to evade phagocytosis. A small number of effectors are associated with the T3SS1 (VP1680, VP1683, VP1686, and VPA450), and these effectors have no homology to any proteins of known function. However, it is predicted that orthologues of some of these effectors will be found in other *Vibrio* species.

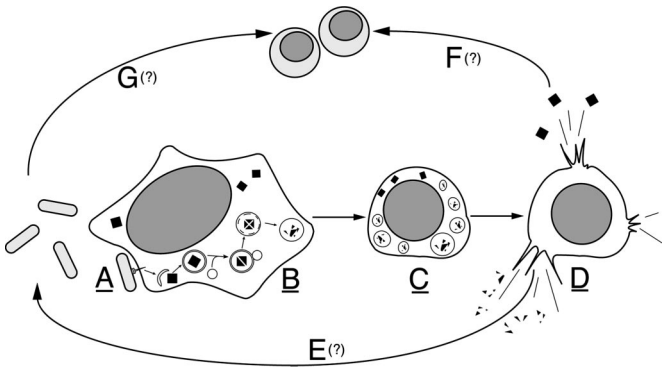

Fig. 5. *V. parahaemolyticus* induces a series of events that culminates in the efficient death of host cells. (*A*) *V. parahaemolyticus* uses a T3SS to inject effectors into a host cell during infection. (*B*) Infection results in the rapid induction of autophagy and the formation of autophagosomes. (*C*) Next, we observe rounding and shrinkage of the infected host cell. (*D*) Rounding and shrinking is followed by cell lysis and release of cellular contents. (*E*) We hypothesize that lysis will lead to the release of degraded proteins that can be used by the bacteria for nutrients. (*F*) In addition, the release of inflammatory contents will cause recruitment of innate immune cells, such as macrophages. (*G*) *V. parahaemolyticus* also can target and kill these immune cells, thereby evading an innate immune response. Underlined letters denote mechanisms that have been demonstrated experimentally herein. Letters with question marks denote events that are hypothesized to occur as a result of these mechanisms.

Thus, it is likely that this mechanism of cell death is an example of a more general mechanism that is used by other bacteria.

Autophagy is a pathway used by cells in response to stress, such as nutrient deprivation, to survive (21). This pathway also functions in both innate and adaptive immunity. It has been shown to play a protective role in defense against intracellular pathogens such as *Mycobacterium tuberculosis*, *Shigella spp*., and many others (27). A host cell can use autophagy to prevent the cytoplasmic replication or invasion of intracellular pathogens by engulfing the pathogens in autophagic vesicles and targeting them to lysosomes (28). In addition, recent work has shown that autophagy may provide defense against a secreted toxin from the noninvasive pathogen *Vibrio cholerae* (29). Alternatively, pathogens have evolved ways to usurp this pathway for their own benefit: for example, the intracellular pathogen *Coxiella burnettii* creates a replicative niche within autophagosomes where it can multiply and survive (30). In contrast, *Shigella flexneri* disrupts phagocytosis and escapes into the cytosol. The pathogen then avoids clearance by autophagy through the type III secretion of an effector protein, IcsB, that prevents recruitment of Atg5, a protein necessary for autophagy (31). In the case of *V. parahaemolyticus*, nutrients released by the infected cell could be used by the pathogen to support its own proliferation. Alternatively, this extracellular pathogen might benefit from inducing autophagy because common intracellular machinery that is used for both autophagy and phagocytosis might be directed away from the host cell membrane, thereby crippling phagocytosis in the infected host cell (32).

Pathogens use a wide variety of mechanisms to exploit a host cell during infection. Herein, we have described a paradigm whereby an infected cell is directed by a T3SS to induce autophagy and cause cell rounding and release of its cellular contents. We observe that inhibition of autophagy does not prevent the eventual death of the infected cell. This result in not surprising in light of what is known about the redundant mechanisms used by T3SSs. For example, *Yersinia spp.* disable the actin cytoskeleton in the host cell by using at least four different mechanisms (6). We have observed that in the *V. parahaemolyticus* T3SS1 multiple mechanisms are used to compromise cell integrity, thereby ensuring the demise of the infected host cells. Future studies of the molecular targets that are hijacked by the effectors secreted by *V. parahaemolyticus* T3SS1 will provide further insight into this orchestrated host-cell death.

Materials and Methods

Cell Lines. HeLa cells were cultured in DMEM (Invitrogen) with 10% cosmic calf serum (HyClone). The GFP-LC3–stable HeLa cell line was generated by inserting GFP-LC3 from GFP-LC3–expressing plasmid, pEGFP-C1 (22), between the NheI and EcoRI sites in the pIRESneo3 vector (Clontech) and selecting for stably expressing colonies with G418 (100 μg/ml) (Gibco). GFP-LC3 HeLas were cultured in DMEM with 10% FBS (HyClone) and nonessential amino acids (Invitrogen). RAW 264.7 macrophages were cultured in DMEM with 10% FBS and 10 mM L-glutamine.

T3SS-Inducing Conditions. T3SS of *V. parahaemolyticus* was induced by growing cultures in LB plus 3% NaCl (MLB) overnight, then diluting the cultures 1:15 into fresh MLB plus 10 mM Na-oxalate and 10 mM $MgCl_2$. Cultures were grown at 37°C for 3 h before infection. T3SS induction of *Yersinia* cultures was performed as described (15).

Infections. HeLa cells or RAW 264.7 macrophages were plated at 0.1×10^6 or 0.5×10^6 cells/ml, respectively, unless otherwise noted 1 day before infection. For microscopy, cells were plated onto sterile glass coverslips. *V. parahaemolyticus* and *Y. pseudotuberculosis* were added to the cells at an MOI of 10 and 100, respectively. Wortmannin (Sigma) was added as a PI3 kinase inhibitor for infection studies. Cell monolayers and bacteria were centrifuged at $500 \times g$ for 5 min at the onset of each infection. Cells were harvested for analysis via Western blot by the addition of 200 μl of SDS sample buffer to each well.

Preparation of Samples for Microscopy. HeLa or RAW 264.7 macrophage cell lines plated on glass coverslips were fixed at indicated time points in 3.2% paraformaldehyde in 1× PBS for 10 min and permeabilized in 0.1% Triton X-100 in 1× PBS for 5 min at room temperature. Cells were stained for actin with rhodamine phalloidin (Molecular Probes) and DNA with Hoechst (Sigma) in 1% BSA and 1× PBS for 20 min at room temperature followed by two washes in 1X PBS. Slides were mounted in 10% glycerol plus *N*-propyl gallate and sealed with clear nail polish.

Visualization of Samples Using Confocal Microscopy. Samples were visualized with a Zeiss LSM 510 scanning confocal microscope. Images were converted by using ImageJ software and Adobe Photoshop.

Measurement of Apoptosis in Infected Cells. Raw 264.7 macrophages were left untreated, infected with POR3 or YP126 as described, or treated with 1 μM staurosporine for 4 h. Cells were lysed and normalized for protein content. Caspase 3/7 activity of 40 μg of protein was measured by the Caspase-Glo assay (Promega). Results are expressed as relative luciferase units. For analysis of PARP cleavage, RAW 264.7 macrophages were treated as described and lysed at the indicated time points in PARP sample buffer (62.5 mM Tris-HCl, pH 6.8, 6 M urea, 2% SDS, 5% β-mercaptoethanol, 10% glycerol, 0.00125% bromophenol blue). Samples were sonicated for 15 s, separated by SDS/PAGE, and immunoblotted with anti-PARP antibody (Cell Signaling) and anti-aldolase antibody (Santa Cruz Biotechnology) to confirm equal loading.

Measurement of LDH Release During POR3 Infection. RAW264.7 macrophages were infected as described over a 4-h time course. Cells were left untreated, infected with YP126 as described, or treated with 1 μM staurosporine as controls. LDH release was measured with a Cytotoxicity Detection kit (Takara). Results are expressed as cytotoxicity calculated as percent of total lysis of cells lysed in Triton X-100.

Electron Microscopy. Cultured cells were fixed in 2.5% glutaraldehyde in 0.1 M sodium cacodylate buffer, followed by 1% osmium tetroxide in 0.1 M sodium cacodylate buffer. After solvent dehydration, centrifuged pellets of cells were embedded in epoxy resin (EMBED 812, Electron Microscopy Sciences) and polymerized at 60°C. Ultrathin sections were cut at a nominal thickness of 80 nm, picked up on copper grids, and stained with uranyl acetate and lead citrate. Sections were examined at 120 kV with a Tecnai G2 Spirit transmission electron microscope (FEI Company), and images were recorded on a Gatan USC1000 2k CCD camera.

Methods for Monitoring Autophagy. To induce starvation, cells were incubated in Hank's balanced salt solution (Invitrogen) in the presence of 10 μg/ml pepstatin A and 10 μg/ml E64-d (Sigma). Samples were probed with anti-LC3

antibody (Novus) or anti-GFP antibody (Invitogen). Relative LC3-II accumulation was determined by quantitating band intensity using ImageJ software and calculating the ratio of LC3-II to LC3-I. The PI3 kinase inhibitor wortmannin (Sigma) was used at 10 μM.

ACKNOWLEDGMENTS. We thank Drs. Tetsuya Iida and Takeshi Honda (Osaka University, Osaka) for their generosity in supplying the *Vibrio* strains; Drs. Joe Goldstein, Melanie Cobb, and Neal Alto for critical reading and helpful discussions; Dr. Beth Levine, Dr. Michelle Laskowski-Arce, Laurie Mueller, and members of the K.O. laboratory for their kind support. K.O., D.L.B., and M.L.Y. are supported by National Institutes of Health-AID Grants R01-AI056404 and R21-DK072134 and Grant I-1561 from the Welch Research Foundation. K.O. is a Burroughs Wellcome Investigator in Pathogenesis of Infectious Disease and a W.W. Caruth, Jr. Biomedical Scholar.

1. Daniels NA, *et al.* (2000) *Vibrio parahaemolyticus* infections in the United States, 1973–1998. *J Infect Dis* 181:1661–1666.
2. Morris JG Jr., Black RE (1985) Cholera and other vibrioses in the United States. *N Engl J Med* 312:343–350.
3. Park KS, *et al.* (2004) Cytotoxicity and enterotoxicity of the thermostable direct hemolysin-deletion mutants of *Vibrio parahaemolyticus*. *Microbiol Immunol* 48:313–318.
4. Ghosh P (2004) Process of protein transport by the type III secretion system. *Microbiol Mol Biol Rev* 68:771–795.
5. Mukherjee S, Hao YH, Orth K (2007) A newly discovered post-translational modification—the acetylation of serine and threonine residues. *Trends Biochem Sci* 32:210–216.
6. Navarro L, Alto NM, Dixon JE (2005) Functions of the *Yersinia* effector proteins in inhibiting host immune responses. *Curr Opin Microbiol* 8:21–27.
7. Park KS, *et al.* (2004) Functional characterization of two type III secretion systems of *Vibrio parahaemolyticus*. *Infect Immun* 72:6659–6665.
8. Liverman AD, *et al.* (2007) Arp2/3-independent assembly of actin by *Vibrio* type III effector VopL. *Proc Natl Acad Sci USA* 104:17117–17122.
9. Trosky JE, *et al.* (2007) VopA inhibits ATP binding by acetylating the catalytic loop of MKKs. *J Biol Chem* 282:34299–34305.
10. Makino K, *et al.* (2003) Genome sequence of *Vibrio parahaemolyticus*: A pathogenic mechanism distinct from that of *V cholerae*. *Lancet* 361:743–749.
11. Bhattacharjee RN, *et al.* (2006) VP1686, a *Vibrio* type III secretion protein, induces toll-like receptor-independent apoptosis in macrophage through NF-kappaB inhibition. *J Biol Chem* 281:36897–36904.
12. Ono T, *et al.* (2006) Identification of proteins secreted via *Vibrio parahaemolyticus* type III secretion system 1. *Infect Immun* 74:1032–1042.
13. Zhang Y, Ting AT, Marcu KB, Bliska JB (2005) Inhibition of MAPK and NF-kappa B pathways is necessary for rapid apoptosis in macrophages infected with *Yersinia*. *J Immunol* 174:7939–7949.
14. Thorburn A (2008) Apoptosis and autophagy: Regulatory connections between two supposedly different processes. *Apoptosis* 13:1–9.
15. Monack DM, Mecsas J, Ghori N, Falkow S (1997) *Yersinia* signals macrophages to undergo apoptosis and YopJ is necessary for this cell death. *Proc Natl Acad Sci USA* 94:10385–10390.
16. Festjens N, Vanden Berghe T, Vandenabeele P (2006) Necrosis, a well orchestrated form of cell demise: Signalling cascades, important mediators and concomitant immune response. *Biochim Biophys Acta* 1757:1371–1387.
17. Brennan MA, Cookson BT (2000) Salmonella induces macrophage death by caspase-1-dependent necrosis. *Mol Microbiol* 38:31–40.
18. Dong Z, Saikumar P, Weinberg JM, Venkatachalam MA (1997) Internucleosomal DNA cleavage triggered by plasma membrane damage during necrotic cell death. Involvement of serine but not cysteine proteases. *Am J Pathol* 151:1205–1213.
19. Fink SL, Cookson BT (2006) Caspase-1-dependent pore formation during pyroptosis leads to osmotic lysis of infected host macrophages. *Cell Microbiol* 8:1812–1825.
20. Mejia E, Bliska JB, Viboud GI (2008) Yersinia controls type III effector delivery into host cells by modulating Rho activity. *PLoS Pathog* 4:e3.
21. Levine B, Yuan J (2005) Autophagy in cell death: An innocent convict? *J Clin Invest* 115:2679–2688.
22. Kabeya Y, *et al.* (2000) LC3, a mammalian homologue of yeast Apg8p, is localized in autophagosome membranes after processing. *EMBO J* 19:5720–5728.
23. Kabeya Y, *et al.* (2004) LC3, GABARAP, and GATE16 localize to autophagosomal membrane depending on form-II formation. *J Cell Sci* 117:2805–2812.
24. Tanida I, Ueno T, Kominami E (2004) LC3 conjugation system in mammalian autophagy. *Int J Biochem Cell Biol* 36:2503–2518.
25. Petiot A, *et al.* (2000) Distinct classes of phosphatidylinositol 3′-kinases are involved in signaling pathways that control macroautophagy in HT-29 cells. *J Biol Chem* 275:992–998.
26. Powis G, *et al.* (1994) Wortmannin, a potent and selective inhibitor of phosphatidylinositol-3-kinase. *CancerRes* 54:2419–2423.
27. Levine B, Kroemer G (2008) Autophagy in the pathogenesis of disease. *Cell* 132:27–42.
28. Levine B, Deretic V (2007) Unveiling the roles of autophagy in innate and adaptive immunity. *Nat Rev Immunol* 7:767–777.
29. Gutierrez MG, *et al.* (2007) Protective role of autophagy against *Vibrio cholerae* cytolysin, a pore-forming toxin from *V. cholerae*. *Proc Natl Acad Sci USA* 104:1829–1834.
30. Kirkegaard K, Taylor MP, Jackson WT (2004) Cellular autophagy: Surrender, avoidance and subversion by microorganisms. *Na Rev* 2:301–314.
31. Ogawa M, *et al.* (2005) Escape of intracellular *Shigella* from autophagy. *Science* 307:727–731.
32. Sanjuan MA, *et al.* (2007) Toll-like receptor signalling in macrophages links the autophagy pathway to phagocytosis. *Nature* 450:1253–1257.